Ref 9

PROCEEDINGS

of the

International Society for Magnetic Resonance in Medicine

SIXTH SCIENTIFIC
MEETING AND EXHIBITION

Sydney, Australia
April 18 – 24, 1998

Volume 2

Fiber-Tractography via Diffusion Tensor MRI (DT-MRI)

Peter J. Basser
Section on Tissue Biophysics and Biomimetics, NICHD, NIH, Bethesda, MD

Purpose

To propose a methodology to calculate continuous fiber-tract trajectories from measured diffusion tensor MRI data, and a rationale for determining fiber tract continuity.

Introduction

In normal and pathological tissues, fiber tract trajectories would provide valuable new microstructural information. In aging and development it would provide a means to follow changes in fiber-architecture. DT-MRI (1) is now the first noninvasive imaging modality capable of generating such fiber-tract trajectories. This is because in each voxel, the fiber tract direction is parallel to the eigenvector, ε_1, associated with the largest eigenvalue, λ_1, of the local diffusion tensor, $\underline{\mathbf{D}}$ (1). However, ε_1 measured by DT-MRI are inherently discrete, noisy, voxel-averaged estimates of the "true" direction vectors (2). To date, it has not been feasible to reconstruct continuous fiber tract trajectories from the measured ε_1. However, a new, efficient $\underline{\mathbf{D}}$-field processing methodology that we just developed, generates a continuous diffusion tensor field, $\underline{\mathbf{D}}(\mathbf{x})$, from measured DT-MRI data (3) from which a continuous ε_1-field map can be calculated. Then, the method below can be used to calculate fiber tract trajectories, and assess fiber tract continuity.

Theory

The fiber tract trajectory vector, $\mathbf{r}(s)$, is parameterized by arc length, s. We solve the linear forced vector differential equation on the left below for $\mathbf{r}(s)$ (4):

$$\frac{d\mathbf{r}(s)}{ds} = \mathbf{t}(s); \quad \mathbf{t}(s) = \varepsilon_1(\mathbf{r}(s))$$

The key new idea presented on the right above is to equate the normalized eigenvector of $\underline{\mathbf{D}}(\mathbf{r}(s))$, $\varepsilon_1(\mathbf{r}(s))$, (associated with the largest eigenvalue of $\underline{\mathbf{D}}(\mathbf{r}(s))$, $\lambda_1(\mathbf{r}(s))$, and the unit vector, $\mathbf{t}(s)$, tangent to the fiber tract trajectory vector, $\mathbf{r}(s)$.

Methods

Numerical methods must be used to obtain $\mathbf{r}(s)$ from $\underline{\mathbf{D}}(\mathbf{x})$. Starting at a point $\mathbf{x}_0$ on $\mathbf{r}(s)$, we evaluate $\underline{\mathbf{D}}(\mathbf{x}_0)$, calculate $\varepsilon_1(\mathbf{x}_0)$ (which is parallel to the slope of $\mathbf{r}(s)$ at $\mathbf{x}_0$), and approximate the position of a nearby point on $\mathbf{r}(s)$, $\mathbf{x}_1$, using a Taylor series expansion of $\mathbf{x}$ about $\mathbf{x}_0$: $\mathbf{x}_1 = \mathbf{x}_0 + \delta\mathbf{x}$ ... Since the correction, $\delta\mathbf{x}$ is parallel to the fiber tract direction at $\mathbf{x}_0$, $\delta\mathbf{x} = \alpha\, \varepsilon_1(\mathbf{x}_0)$, where α is a (small) constant. These steps are repeated for a new point, $\mathbf{x}_1$; the process is then iterated. This is Euler's method. While easy to implement, there is no way to correct its prediction of $\mathbf{r}(s)$, leading to accumulated errors (5). However, using our continuous representation of $\underline{\mathbf{D}}(\mathbf{x})$, we can now calculate second and higher derivatives of $\varepsilon_1(\mathbf{x})$ at any point, and thus improve accuracy by employing higher order correction schemes, e.g., Runge-Kutta methods (5).

Results

To test their fidelity and spatial frequency response, a family of analytical 3-d $\underline{\mathbf{D}}(\mathbf{x})$ maps was synthesized with fiber tract direction fields having a (a) non-zero divergence (converging or diverging fiber pattern), (b) non-zero curl (circulating, open or closed fiber pattern), or (c) periodic or uniform fiber directional pattern. Fig 1 shows a fiber tract trajectory, $\mathbf{r}(s)$, calculated from such a test map in which all three Euler angles of $\underline{\mathbf{D}}(\mathbf{x})$: $\phi(\mathbf{x})$, $\varphi(\mathbf{x})$, and $\theta(\mathbf{x})$, varied continuously through the image volume.

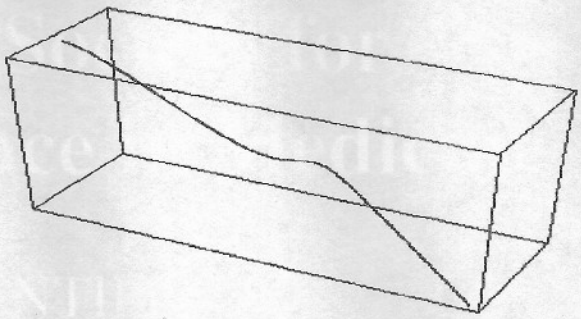

Fig 1. Computed 3-d fiber tract trajectory from synthetic $\underline{\mathbf{D}}(\mathbf{x})$ image.

Predictably, however, we were unable to follow the fiber-tract trajectory through singularities (sources or sinks) in the fiber direction field. Closed and open fiber paths could be followed reliably, though, provided that the step size was small compared to the local radii of curvature.

Discussion and Concluding Remarks

Two paradigmatic problems arise in this emerging field of *DT-MRI Fiber Tractography* in trying to assess fiber-tract continuity or functional connectivity. One is an initial value problem--to follow a fiber trajectory starting from one point on it. Another is a two-point boundary value problem--to establish whether two points (or regions) are connected by a single fiber-tract (or set of fiber tracts). Note, if these regions are connected by fiber tracts that cross, branch, merge or fan out, causing "powder averaging" of the $\underline{\mathbf{D}}$-field at these points (6), then without additional *a priori* or *a posteriori* information about the distribution of fiber tract directions within these voxels, tracing fibers through them is problematic. In functional PET and MRI studies, "activity" is often reported simultaneously in different brain regions following stimulation. Here, it is naive to imagine that DT-MRI alone can provide an anatomical basis for simultaneous activation by establishing connections between these regions via gross neural pathways. Nevertheless, using the new methodology presented here, determining fiber trajectories in large coherently oriented white matter tracts, such as the spinal cord, corpus callosum, and pyramidal tracts, as well as in other ordered soft tissues, is now feasible.

References

1. Basser, PJ et al., *Biophys. J.*, 66, 259-267, 1994.
2. Basser, PJ et al., *J. Magn. Reson*, B 103, 247-54, 1994.
3. Aldroubi, A et al, in prep., 1998.
4. Kreyszig, E, *Differential Geometry*, 1991.
5. Press, WH et al., *Numerical Recipes in C*, 1992.
6. Pierpaoli, C et al., *Magn. Reson. Med.*, 36, 893, 1996.